Advances in Forest Fire Research 2018

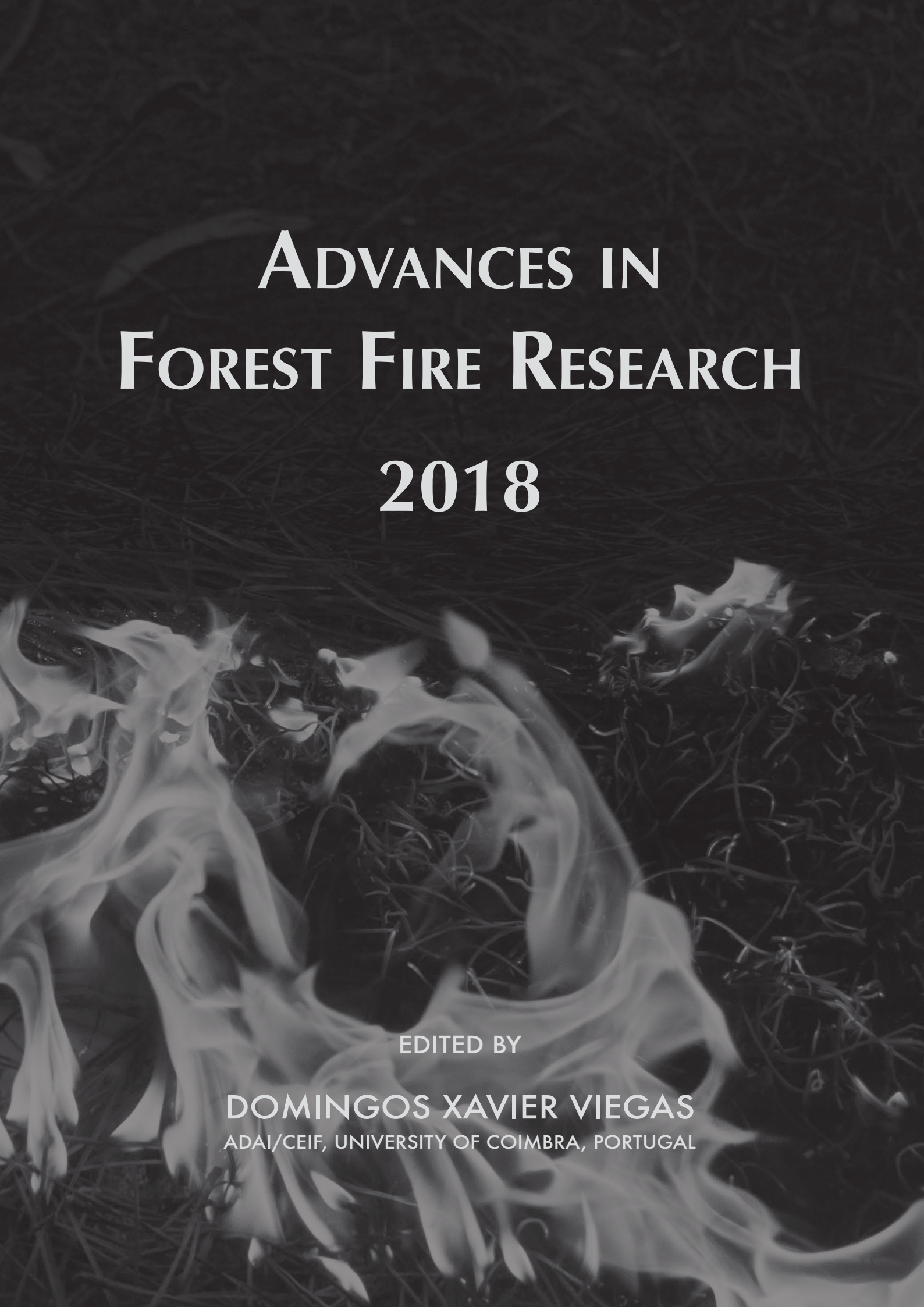

EDITED BY

DOMINGOS XAVIER VIEGAS

ADAI/CEIF, UNIVERSITY OF COIMBRA, PORTUGAL

Advances in Forest Fire Research 2018 - D. X. Viegas (Ed.)
Chapter 4 – Fire at the Wildland Urban Interface
https://doi.org/10.14195/978-989-26-16-506_90

Modelling fire spread and damage in wildland-urban interfaces

Fabien Fernandez[1*]; Bruno Guillaume[1]; Bernard Porterie[2]; Anne Ganteaume[3]; Fabien Guerra[3]

[1]*ARIA Technologies. 8/10, rue de la Ferme - 92100 Boulogne-Billancourt, France {ffernandez@aria.fr*}*

[2]*Aix-Marseille Université, CNRS, IUSTI UMR7343, Marseille {bernard.porterie@polytech.univ-mrs.fr }*

[3]*IRSTEA Aix-en-Provence {anne.ganteaume@irstea.fr }*

Abstract

Fires in wildland-urban interfaces (WUIs) are currently increasing because of the urban sprawl entailing larger contact zones with wildland areas and the on-going climate change, increasing the frequency and severity of extreme fires, especially in Mediterranean ecosystems. Heterogeneous vegetation in the WUIs, including both natural and ornamental species, allows the fire to propagate from the wildland to housing, which can be responsible for loss of life and considerable property and environmental damages. In the present study, the raster-based fire spread model SWIFFT (De Gennaro et al., 2017) is enhanced to account for fire-induced thermal damages on vegetation and building materials at the WUI. This approach is applied to two historical WUI fires. It is found that the enhanced model is particularly well suited first, to assess the changes in fire behavior, as the fire travels from the natural to the ornamental vegetation, and, second, to estimate damages on buildings. It can also be used to evaluate the effectiveness of fuel treatment strategies on wildfire exposure at the WUI scale, depending on local conditions of wind, topography and vegetation.

Keywords: Forest fire, raster-based fire spread model, wildland-urban interface, WUI, fuel treatments, building vulnerability

1. Introduction

Significant efforts have been made in the past to provide insights into the pattern of development and expansion of fires at the wildland urban interface (WUI) (Cohen 2000, Cohen 2008), which revealed that the wildland urban interface is a house ignitability problem and not a wildland fire control problem.

Among the many fire spread models (see Sullivan, 2009), only a few have been applied to the WUI problem. There are two main reasons for this. First, the WUI vegetation differs significantly from that of wildland areas as it is composed of a mix of wild and ornamental plant species, generally the latter surrounding buildings. Second, most fire spread models are based on the assumption of fuel continuity and homogeneity, which is somewhat questionable at the WUI. CFD physics-based models, like the wildland-urban fire dynamics simulator (WFDS, Mell et al., 2007), or raster-based models (Sullivan, 2009) are thus good candidates to model WUI fire behavior.

The approach described in this paper aims at bridging this gap, by using a raster-based model inherently designed to model fire patterns in heterogeneous landscapes. The SWIFFT model (De Gennaro et al., 2017) distributes the vegetation on a regular (here, hexagonal) network at a fine resolution. The empirical part of the model provides a description of flammability and combustibility properties of the vegetation items, including canopies. The physical part of the model includes a solid flame model for the burning sites to evaluate radiation and convection effects, as well as an energy conservation equation to describe the thermal degradation (i.e., heating, drying and ignition) of unburnt vegetative elements.

In the current work, SWIFFT is enhanced to model, at a fine scale, the fire propagation through the ornamental vegetation and the fire-induced damages to the vulnerable building materials that can be

found at the WUI. The initial empirical fuel model in SWIFFT is also improved to fine tune the behavior of ground and canopy fuels exposed to fire (Scott and Reinhardt, 2001).

2. Methodology

2.1. Basic SWIFFT model

The starting point of the present approach is the fire spread model called SWIFFT, which considers the local conditions of wind, topography, and vegetation and combines (1) a network model to represent vegetation distribution on land with a given vegetation coverage, (2) an empirical flame model using a single burning fuel element per network site, and (3) a thermal model describing the heat transfers from burning to unburnt vegetation items, by radiation and convection processes. The reader might refer to De Gennaro et al. (2017) for more details.

In SWIFFT, the network model is composed of combustible and non-combustible cells. During a simulation, two neighborhoods are identified for each burning site: a radiation circular neighborhood, which includes all the sites that can be potentially exposed to radiation, and a convection rectangular neighborhood, which contains all the sites that can be potentially located in the wake of the burning site (Figure). Therefore, the thermal response of unburnt fuel elements to heating depends on whether it belongs to the radiation neighborhood, the convection neighborhood, or both. The characteristic length of these neighborhoods is estimated beforehand from numerical trials.

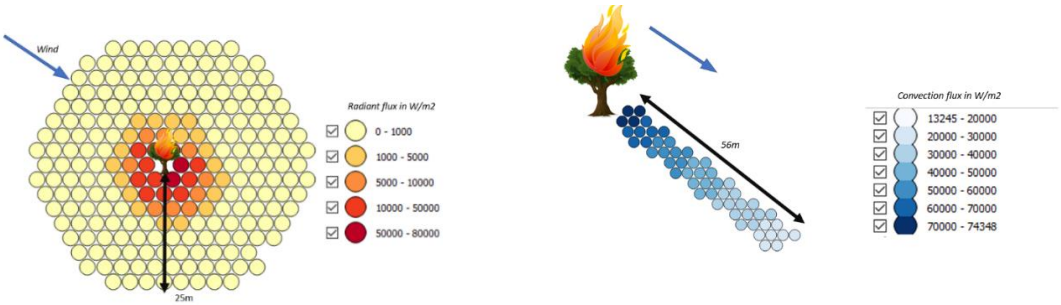

Figure 1 - Radiation neighborhood (left) and convection neighborhood (right) for a flame length of 5.6 m and a wind speed of 10ms-1. Here, the characteristic length of the radiation neighborhood is 25 m, that of the convection neighborhood is ten times the flame length, thus 56 m.

In the proposed version of the SWIFFT model, a hexagonal network of 3-m-diameter sites is used. Unlike amorphous networks (De Gennaro et al., 2017), the location of each site in a two-dimensional regular network can be easily determined using two indexes, which saves computing time.

The fire here is not simulated from its outbreak, but rather by pre-positioning the flame front slightly upstream of the WUI. This can be done empirically or using visual observations from real fires. This initial fire front is represented as a GIS polygon and the fire properties of all the network sites which belong to this polygon are calculated using the empirical flame model of SWIFFT.

2.2. Enhancements from the SWIFFT model

In the original SWIFFT model (De Gennaro et al., 2017), each vegetation site is composed of a single fuel type. Here, we replaced this approach with that of a multi-element fuel scene as in Rothermel et al. (1972). A fuel scene is now described with different constitutive fuel elements: dead fuels, that are referred as 1hr, 10hr, 100hr fuels, depending on their tendency to dry, and live fuels (herbs and shrubs). We also added the canopy fire parameterization proposed by Scott and Reinhardt (2001) to account for the increase in fire intensity and residence time due to passive and potentially active crowning, according to some average properties of canopies (height, base height, bulk density, fuel load). In addition to the default fuel map for natural forests, with a 30m-spatial resolution over the zone of interest, we used additional GIS polygons which are intersected with the site network to more

accurately allocate the fuel types to the sites, for the wildland vegetation, as well as for the ornamental vegetation in the garden. The natural forest vegetation is modelled by a single fuel type in the case studies hereafter, whose combustion properties were kindly provided by the French Forest Service. The combustion properties of canopies (based on the Irstea's fuel database) for the ornamental vegetation of the current case study were determined tree-by-tree in the two case studies.

The weather parameters (wind, temperature, relative humidity and fuel moisture content) are inferred from the nearest weather station. The wind conditions are refined on the local topography at 100m resolution from the local scale air mass-conservative model, WindNinja (Forthofer et al., 2009).

2.3. Coupling SWIFFT with a module of fire-induced thermal degradation of building materials

To account for the thermal degradation of materials, the vulnerable assets are not modelled as 3D structures in the model. Even if Building Intelligent Models are in growing development worldwide in cities, they are still far from being systematically applied currently, and buildings in WUI can still rarely be modelled with their full 3D structure allocations. In the model, a good compromise is found by using GIS (2+0,5)-D polygon objects in the zone of interest, e.g. for each polygon a description is used of (1) a single building height and (2) a list of types of building materials (e.g. glass, wooden construction elements). This nature of information is more largely spread in cities.

Horizontally, the 'vulnerable sites' through the network are identified by crossing the 2D polygon shape with the underlying site network. Vertically, the building's facades are represented as a collection of 1m² panels distributed every 2m in height. Each facade panel can receive heat flux due to radiation from the flames and hot gas. Ignition can occur depending on the thermal properties of panel materials.

The facade height is measured relatively to the flame base height on ground. Normal vectors to the facade panels are also calculated and then used during the simulation to assess the azimuth angle, characterizing the view angle of the panel as seen by a network site from the incoming fire front.

For radiative preheating of the facade panels, as done similarly for the radiative preheating of unburnt vegetation (see De Gennaro et al., 2017), precalculated tables based on Monte Carlo simulations are used. However, for facade panels, additional parameters are introduced in the table pre-calculation: the panel azimuth angle, the output fluxes are provided on a 3D grid providing the preheating at different stock building levels. Figure illustrates the pre-calculated fluxes on two sample cases. Panels located at negative heights are also considered.

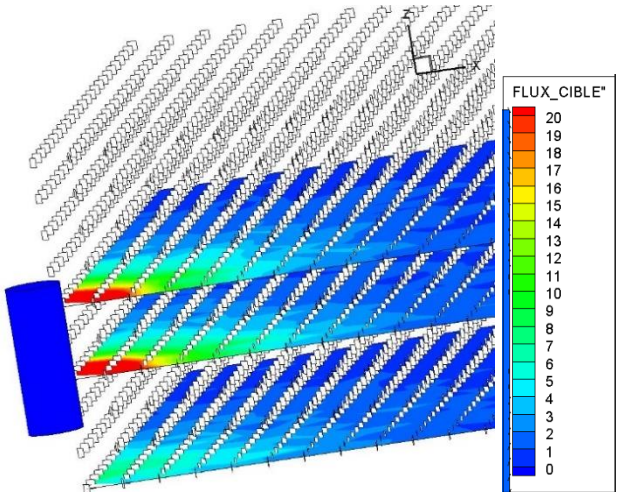

Figure 2 -Sample visualization of pre-calculated radiative fluxes (unit: kWm-2) on the 3D output grid (having resolutions of dx=2m, dy=2m,dz=2m) with one receptor ('facade panel') positioned at each grid cell having fixed azimuth of 15°, for a selected flame (radius=1.5m, length=7m) for a flame angle=0°

For reasons of symmetry, the pre-calculated fluxes are calculated only in the X+, Y+ and Z 3D-subspace. During simulations, the vertical position of the panel height with respect to the flame base takes into account (1) the building stock height at which the panel is located, (2) the building altitude above sea-level and the (3) the flame altitude above sea-level.

For convective preheating of the facade panels, the same rectangular neighborhood is considered as for the convective preheating of the unburnt vegetation. However, the parameterization of the convective heat flux considers the relative vertical position of the panel vs. the flame base.

The case of an active crowning fire is also treated. Therefore, a facade panel can be exposed to the convective fluxes from both surface and canopy burning sites. For the latter, the reference height is taken as half the canopy height.

2.4. SWIFFT outputs

The first output of the model is the area burnt in the vulnerable zone, in both natural and ornamental vegetation. Moreover, the model allows the user to identify which sites exhibit surface to crown fire transition. The damage caused by fire on each material type in the vulnerable zone can be evaluated from the model. It depends on the time evolution of the total incident flux (radiation plus convection), and on the material thermal properties. Two ignition criteria are used, either based on a critical temperature or a critical total heat flux. The latter criterion is retained to model the breakage of double glazing windows. The percentages of panels damaged by fire on each building facade is an another ouput of the model. At this stage of development, fire-induced damage in the interior of houses is not considered.

3. Validation on case studies of WUI impacted by historical fires

This section summarizes the description of the case studies, as well as model results, in terms of fire behavior and chronology while approaching the two vulnerable zones, and damages on the vulnerable assets. In these two case studies, fire spotting risk was found to have no impact on fire spread and structures, so damage came essentially from the convective heat (hot gases) or direct contact with flames. These case studies have been selected because of their extreme behavior, with total burnt areas of 6744ha for the Vidauban fire and 2663ha for the Rognac fire, due to wind speed exceeding 30kmh^{-1}, air relative humidity below 30% and severe drought conditions. For both cases, we detail the fire behavior and chronology, the environmental conditions (topography, fuel and weather) in the vulnerable zones during the events, as well as the precise nature of material types of the vulnerable assets exposed to fire.

3.1. Rognac fire

The Rognac fire occurred in the afternoon of the 10th of August 2016, spread over 2663ha between 3pm and 1am of next day affecting seven communities, especially those of Rognac (where the fire started), Vitrolles and Les Pennes-Mirabeau. When the fire ignited, the firefighting force was limited due to an unexpected firefighting aircraft maintenance that grounded most aircrafts but also to several other fires that burned the same day in nearby locations, including the critical fire in Fos/Mer (more than 1000ha burned) that threatened the oil terminal. These concomitant fire outbreaks caused the splitting of the firefighting force onto different locations and because of this cascade of events, the fire was not contained soon enough as the massive early attack of the fire could not be achieved (usually the fire attack occurs less than 10 minutes after ignition with full force).

The average weather conditions have been reconstituted using data from the nearest meteorological station (i.e. Marseille airport, located less than 2km from the vulnerable zone): wind direction of NW, wind speed of 12m/s in the afternoon, relative air humidity of 25%, ambient air temperature of 30°C. The fine fuel moisture was estimated to 10%.

The local vulnerable zone of the case study presented here is located on the community of Vitrolles (latitude 43.436105 and longitude 5.262842). It was also possible to piece together the local fire chronology, both from the general fire chronology of the whole fire as well as from precisions provided by the damaged house's owner. The fire arrived from the NW (see Figure) and, after crossing a road, it restarted in the small forested groves located 100m downwind the small residential district.

Figure 3 - left: post-fire pattern in the area of interest; middle: G-Earth view with vegetation before the fire (A left view), A right view: view of the cut trees and cleaned zone two years after the fire.

It is worth noting that the understory in the white oak stand (natural vegetation) was reported to be quite dense, since grass residues from a recent cleaning were still laying on the ground. An additional modelling assumption was to use a vegetation coverage of 91%, coherent with the vegetation density as reported on Google-Earth photo before the fire.

We run a simulation of 10 min-duration, with a fire front initially positioned in the northwest corner of the WUI (Figure). The dominant species of the wild vegetation was white oaks. A single type of material, namely the glass simple pane window, is considered. A critical heat flux for glass breakage of 10 kW/m² is used.

A general view of the vulnerable zone is given in Figure 4.

Figure 4 - Rognac fire: visualization of the initial fire front position and the different polygons used to model the natural and ornamental vegetation (in green), non-combustible materials (in grey; swimming-pool, concrete areas, etc.), and combustible material (in orange).

Figure allows the comparison between the observed and the predicted damages. Regarding observed damages, glass breakage occurred on the A1 facade, as reported by the house's owners, leading to an interior fire. Fire propagated from A1 to the ornamental hedge D, as confirmed by the house's owner. From a Google-Earth view after the fire, the ornamental hedges C can be considered

as burnt. The facades of house B were kept intact, and the fire did not propagate to the garden. As shown in Figure , the simulation reproduces well the damages on C and A1 (only 1 on 2 facades), the damages on D, and the no-damages on B. The damaged house A1 was fully exposed to fire due to the continuity from the natural to the ornamental vegetation in the garden. In contrast, the house B was undamaged essentially because it was sheltered from the fire by the damaged house A1, the fire front coming from the NW direction.

The simulated fire propagated throughout the natural vegetation with average spread rate of about 1kmh^{-1}, and average flame length of about 6m.

Figure 5 - Rognac fire: comparison between the observed (left) and predicted damages after 300 s (middle) and 600 s (right) of fire. For the two latter, the red areas correspond to the burning areas, the black ones to the areas burnt due to crowning, and the grey ones to the areas burnt from surface fire. Contour legend gives the percentages of panels damaged by fire on each building facade.

3.2. Vidauban fire

The Vidauban fire occurred on the 17th of July 2003, during a record year regarding heat wave and drought in France. It spread over 6744ha between the city of Vidauban and the Mediterranean Sea, crossing the community of Plan-de-la-Tour, where the studied vulnerable zone is located. The local vulnerable zone presented here is found approximately at location of latitude 43.368216 and longitude of 6.554530. It was possible to piece together the fire relative chronology, not in absolute time, but from its arrival in the studied garden up to when it left the property, because the house's owner had witnessed the fire from inside his house and was able to report the chronology. The fire arrived from the NW in the garden and the fire fighters were not present in this area at that time.

The exact moment of the fire in the vulnerable zone was not reconstituted, and the weather could not be precisely estimated, the nearest Meteo France weather station being too far. We took the average behavior weather conditions from 12am to 6pm as representative of the local weather: wind blowing from the NW (300°) at a speed of about 10ms^{-1}, ambient temperature of 26°C, and air relative humidity of 20%. The fine fuel moisture was estimated at 10%.

Figure 6 - Vidauban fire: two pictures taken after the fire of the WUI at two different angles of view.

The house was not damaged by the crown fire that arrived from the NW thanks to the brush-clearing of the ground vegetation around the house performed by the owner and the effective tree pruning and

thinning, up to 1.80m from the ground level. As can be seen, the vegetation is scorched but not fully burned as is the case for the vegetation outside the garden.

The owner could describe the entire vegetation present just before the fire, some of which is still in place today. He could also describe the damage that occurred to the building materials.

The natural vegetation is the same as in the previous case study, white oak with partly cleaned understory. A vegetation coverage of 91% was also used here, in accordance with owner's observations and the distribution of vegetation that was not burnt by fire in the same area. The individual trees, white oaks, have been approximately described tree-by-tree with the owner. Figure exhibits all modelled zones.

A simulation of 1000s-duration was performed, with a fire positioned according to the fire arrival seen by the owner in the natural vegetation, upstream of the two houses. The house A2 was surrounded by natural vegetation (Figure).

Figure 7 - Vidauban fire: visualization of the initial fire front position and the different polygons used to model the areas covered with natural and ornamental vegetation (in green), those composed of non-combustible (in grey: swimming-pool, concrete areas, etc.) and combustible (in orange) materials.

The observed and predicted damages are shown in Figure . The damages on house A2 are total: the house has been destroyed. The model simulates glass breakage on the two most exposed facades of this house which was in direct contact with the fire. However, the fact that the exterior damage was due to glass breakage is not evident.

Figure 8 - Vidauban fire: comparison between the observed (left) and predicted (middle and right) damages (for color code see caption of Figure).

The model exhibits a strong reduction in fire intensity, when it travels from the natural area to the cleared garden. The spread rate of fire is reduced by 2.5 (2.5 vs. 1kmh^{-1}) and the flame length decreases from 6 to 0.8m. The fire intensity is so much reduced that the trees in the garden do not exhibit any crowning and that the house is undamaged.

It was observed that the house A1 was very slightly damaged, with only exterior damage. This is not reproduced by the model, which suggests that the grass fire intensity is underestimated.

4. Conclusions

The SWIFFT model has been enhanced to simulate fire patterns in the heterogeneous vegetation (both natural and ornamental) and the external damages on building materials at the WUI. This approach has been tested on two WUI historical fires: the Rognac fire in 2016, and the Vidauban fire in 2003, using glass breakage as a good indicator of external damages on buildings. The observed damages and fire patterns are well reproduced by the model. The approach will be used to evaluate, on private properties or at the scale of districts, the effectiveness of fuel treatment in the reduction of fire risk.

5. Acknowledgments

We acknowledge the French Safe Cluster for selecting the project in its Challenge Booster Space4Earth, as well as Climate-KIC for sponsoring this work in the framework of the H2020-OASIS-insurance project. We also thank the owners of the houses in the two case studies who took on their own times to provide us very useful information on the state of the houses and gardens during and after the fire.

6. References

Butler BW, Cohen JD (1998) Firefighter Safety Zones: A Theoretical Model Based on 494 Radiative Heating. *International Journal of Wildland Fire***. 8**. 73–77.

Cohen J (1995), Structure Ignition Assessment Model, USDA Forest Service Gen. Tech. Rep. PSW-GTR-158.

Cohen J (2000) Preventing disaster: Home ignitability in the wildland-urban interface. *Journal of Forestry* **98(**3): 15-21.

Cohen J (2008) The wildland-urban interface fire problem: A consequence of the fire exclusion paradigm. *Forest History Today*. Fall: 20-26.

De Gennaro M, Billaud Y, Pizzo Y, Garivait S, Loraud J-C, El Hajj M, Porterie B (2017) Real-time wildland fire spread modeling using tabulated flame properties. *Fire Safety Journal* **91**, 872-881. doi: 10.1016/j.firesaf.2017.03.006.

Finney MA (2004) FARSITE: Fire Area Simulator–model development and evaluation. *Research Paper RMRS-RP-4 Revised.* Ogden, UT: U.S. Department of Agriculture, Forest Service, Rocky Mountain Research Station.

Forthofer J, Shannon K, Butler B (2009) Simulating diurnally driven slope winds with WindNinja, in Proceedings of 8th Symposium on Fire and Forest Meteorological Society.

Mell W, Jenkins MA, Gould J, Cheney P (2007) A physics-based approach to modeling grassland fires. 2007. *International Journal of Wildland fire*. **16**(1): 1-22.

Porterie B, Zekri N, Clerc JP, Loraud JC (2007) Modeling forest fire spread and spotting process with small world networks. Combustion and Flame – *Combust. Flame*, **149**. 63-78. doi: 10.1016/j.combustflame.2006.12.008.

Rothermel RC (1972) A mathematical model for predicting fire spread in wildland fuels. Res. *Pap. INT-115*. Ogden, UT: U.S. Department of Agriculture, Intermountain Forest and Range Experiment Station. 40 p.

Sullivan A (2009) Wildland surface fire spread modelling, 1990–2007. 1: Physical and quasi-physical models. *International Journal of Wildland Fire*. **18**. 349-368. 10.1071/WF06143.